Available online at www.sciencedirect.com
SCIENCE DIRECT®
Estuarine, Coastal and Shelf Science 65 (2005) 123–134
ESTUARINE COASTAL AND SHELF SCIENCE
www.elsevier.com/locate/ECSS

Spatial characteristics of sediment trace metals in an eastern boundary upwelling retention area (St. Helena Bay, South Africa): A hydrodynamic–biological pump hypothesis

Pedro M.S. Monteiro [a,b], Alakendra N. Roychoudhury [c,*]

[a] *Department of Oceanography, University of Cape Town, Rondebosch 7700, South Africa*
[b] *Coast Programme, CSIR, P.O. Box 320, Stellenbosch 7599, South Africa*
[c] *Department of Geological Sciences, University of Cape Town, Rondebosch 7700, South Africa*

Received 28 September 2004; accepted 19 May 2005
Available online 15 July 2005

Abstract

St. Helena Bay, a retention zone located in the southern Benguela upwelling system, is an important fish nursery. However, it suffers from seasonal bottom water hypoxia causing major economic losses. Anoxic conditions are linked to sulfide fluxes from bottom sediments defined by a high sedimentation rate of organic matter. It is proposed that trace metals may play an important role in alleviating part of the ecological stress by forming sulfide complexes in such systems. A spatially intensive data set of sediment biogeochemical characteristics showed that POC and trace metals (Cr, Cu, Zn, Ni, etc.) accumulated in the central zone of the Bay. Furthermore, trace metal concentrations were strongly correlated with both POC and Al. To explain the observed biogeochemical relationships in St. Helena Bay, we propose a hypothesis that links the upwelling retention hydrodynamics, primary productivity and sediment trace metal distribution. Trace metals are incorporated into phytoplankton cells in the euphotic zone but rapidly sediment along with particulate organics, on their senescence. Both, the biological pump and the dispersion of particulates are primarily controlled by the hydrodynamics prevalent within St. Helena Bay, which also govern the retention zone in the shadow of one of the major upwelling cells. The dynamics of entrainment–stratification drives the productivity, while a residual cyclonic gyre concentrates the surface productivity within the bay. Bed-shear stresses spatially constrain the accumulation of biogenic organic matter, which governs the trace metal biogeochemistry of the sediments, along a narrow terrigenous mud belt.

Keywords: Benguela upwelling ecosystem; dispersion; hydrodynamics; primary production; St. Helena Bay; trace metals

1. Introduction

Retention zones in the shadow of upwelling centers in eastern boundary upwelling systems are now known to play key ecosystem regulation roles. These include, productive nurseries to early life stages of fish (Bakun, 1998), areas of formation and incidence of harmful algal blooms (Pitcher et al., 1992, in press; Probyn, 1992) and coastal hypoxia (Bailey, 1991; Chapman and Bailey, 1991; Monteiro and van der Plas, in press). While the ecological importance of retention areas in general and St. Helena Bay in particular (Hutchings, 1992; Roy, 1998) has been recognized, their role in the development and maintenance of organic rich sediments and coupled elemental cycling is less well understood.

Underlying the ecosystem roles of retention zones are the complex hydrodynamic processes that govern the recirculation and stratification, and upwelling and sedimentation – re-suspension characteristics (Jones et al.,

* Corresponding author.
E-mail address: aroy@geology.uct.ac.za (A.N. Roychoudhury).

0272-7714/$ - see front matter © 2005 Elsevier Ltd. All rights reserved.
doi:10.1016/j.ecss.2005.05.013

1998; Monteiro and Largier, 1999; Penven et al., 2000). St. Helena Bay in the southern Benguela upwelling system has the hydrodynamic characteristics typical of retention areas lying "downwind" or equatorward from an upwelling Cape in eastern boundary current systems. It shares a number of hydrodynamic, biogeochemical and ecological properties with comparable systems (Shannon, 1985; Chapman and Bailey, 1991; Hutchings, 1992) such as, Monterey Bay, California (Nelson and Hutchings, 1983; Shannon, 1985; Graham and Largier, 1997; Penven et al., 2000). Although St. Helena Bay is nitrogen limited (Chapman and Bailey, 1991), the retention zone is characterized by chlorophyll-*a* concentrations that are higher than what is expected from new production alone (>15 mg Chl m^{-3}) and peaks at 68–139 mg Chl m^{-3} (Bailey, 1987; Pitcher et al., 1989, 1992). This contributes to the high sediment flux (31.5 g m^{-2} d^{-1}) observed in the bay area (Bailey, 1987). Sediment sulfide fluxes are coupled to the sedimentation of ageing phytoplankton blooms, which then enhances the hypoxic character of sub-thermocline waters. Off the west coast of South Africa between St. Helena Bay and Elands Bay, regular episodes of oxygen depletion within the coastal ocean waters have been witnessed in the late summer (Chapman and Shannon, 1985; Monteiro and van der Plas, in press). These hypoxic conditions are maintained throughout the St. Helena Bay area as a result of the combined effects of stratification, retention and remineralization of carbon export fluxes (Monteiro and van der Plas, in press). Hypoxic conditions coupled with elevated near bottom sulfide concentrations have, in the past, resulted in major mortality events for organisms such as rock lobsters, fish and mussels, thereby causing significant economic losses (Cockroft et al., 2000).

Metals, trace or major, in such a system may play a vital ecological role, providing a potential remediation by forming complexes with free sulfide and alleviating part of the ecosystem stress. Furthermore, because of the ecological significance and the pollution potential of trace metals, it is important to understand processes responsible for mobilization or entrapment of nutrients and trace metals in organic rich retention zones associated with upwelling systems. A number of studies have investigated the role of organic matter and other biogeochemical factors in trace metal accumulation and distribution in coastal regions (Noriki et al., 1985; Wangersky, 1986; Fisher and Wente, 1993; Hudson and Morel, 1993; González-Dávila, 1995; Löscher, 1999; Whitfield, 2001; Vasconcelos et al., 2002; Morel and Price, 2003). Furthermore the links between hydrodynamics, specifically current and wave stress driven sedimentation – re-suspension processes, and trace metal accumulation have also been recognized and better understood in certain coastal environments (Le Gall et al., 1999). However, less is known of the process scales that govern the unique linkages between the hydrodynamic forcing that result in the development of retention areas, and thus, organic matter and trace metal rich repositories, within an upwelling zone.

In this study we use a spatially comprehensive data set of sediment trace metals, organic matter (POC and PON) and stable isotopes ($\delta^{13}C$ and $\delta^{15}N$) from the St. Helena Bay retention area together with recent modeling and observational understanding to propose a hypothesis that links hydrodynamics and new production to the sequestration of trace metals in the sediments and, ultimately, their fate.

2. Materials and methods

2.1. Site description

Sediment samples were collected in and around St. Helena Bay off the west coast of South Africa in the late summer of 2001 (Fig. 1). St. Helena Bay is a semi-enclosed, shallow (depth < 100 m) bay, east of Cape Columbine (Fig. 1b). Cape Columbine has been identified as one of the main upwelling centers in the southern Benguela upwelling system and it exerts a considerable control over the biogeochemical characteristics of the St. Helena Bay. Upwelled waters flow north northwestward off Cape Columbine (Shannon and Nelson, 1996), however, a sluggish cyclonic gyre is often observed (Chapman and Bailey, 1991; Touratier et al., 2003). In addition, close to the coast, the subsurface flow is often polewards (Shannon, 1985). On a short-term scale, the hydrography within the bay can be complex and strongly modulated by the event scale (Shannon, 1985).

Sediments in the bay are primarily brought in either as atmospheric input or carried by the Berg River (Fig. 1). Offshore fine-grained sediments from as far north as the mouth of the Orange River are also known to be transported to St. Helena Bay along with the subsurface southward current (Bremner et al., 1990; Rogers and Bremner, 1991). The Berg River and its tributaries primarily flow through areas dominated by agriculture, wineries, canneries and textile milling (Fourie and Steer, 1971). In the upper reaches, Berg River flows mainly through the Table Mountain Group Sandstone, granitic hills and clay soils consisting of weathered granitic material. Downstream, the sandstones have been eroded to expose Malmesbury Group shales that form the underlying bedrock for the remaining part of the river channel to the mouth (Fourie and Steer, 1971).

2.2. Sediment collection and characterization

Surface sediments were collected from 37 sites throughout the bay and the mouth of the Berg River

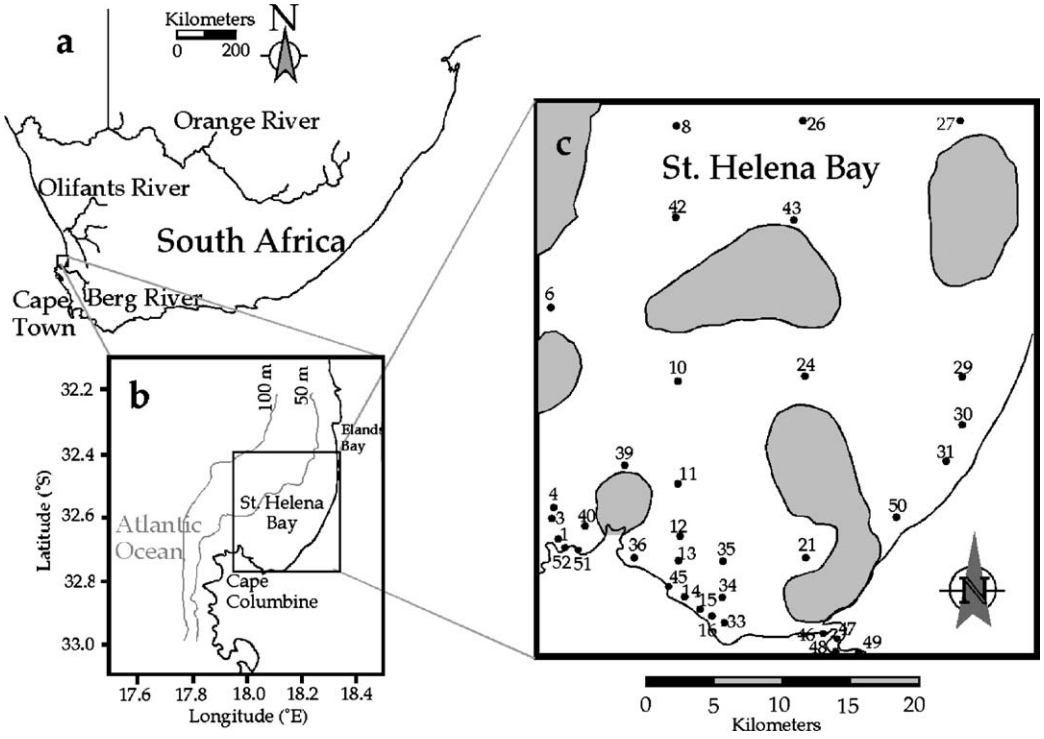

Fig. 1. (a) Site location (b) details of St. Helena Bay region and local bathymetry and (c) location of sampling points. The gray filled areas denote the extent of calcareous reefs.

using a multicorer, a Van Veen grab sampler or hand held corers by divers as dictated by conditions (Fig. 1c, Table 1). Immediately after collection, each sample was sectioned in two parts (0–5 cm and 5–10 cm), bagged and transported to the laboratory on ice. At the laboratory, one fraction of the sediment samples was thawed and air-dried under nitrogen for further analyses. Grain-size analyses were performed by sieving to separate gravel, sand and mud fraction.

2.3. Bulk trace metal concentrations

Porewaters from 0 to 5 cm fraction of each sediment sample were removed by forcing nitrogen gas through them. Following this, the samples were oven-dried at 105 °C and ground in an agate mortar and pestle. Ground sediment (0.25 g) was weighed and transferred into a 30 ml Teflon® vessel. The sediments were subjected to acid digestion (5 ml conc. HNO_3 + 1 ml $HClO_3$ + 1 ml H_2O_2) in a microwave digester. If required, the digested samples were diluted with trace pure HNO_3 and analyzed for trace metals using an ICP-AES.

2.4. Carbon and nitrogen analyses

The carbon and nitrogen contents of the sediments were determined using a CHN-analyzer (Carlo Erba 2500). Total carbon and nitrogen content was measured simultaneously by combusting 5 mg of dried and ground sediment sample. For organic carbon, 0.3 g of the individual sediment samples was first treated with 2 ml of 16% HCl to completely remove the carbonates. The samples were allowed to dry in an oven at 40 °C. Subsequently the salts were removed by washing the samples with 5 ml of 1 M ammonium formate. The slurry was filtered and sediments dried once more at 40 °C. The dried sediments were ground in an agate mortar with an agate pestle and 5 mg of sediment was placed in an aluminum boat for analysis using the elemental analyzer.

The $\delta^{13}C_{PDB}$ of organic carbon was determined by first treating the dry sediments with HCl as described above. The isotopic ratios were determined on 5 mg of decalcified samples using a Carlo Erba elemental analyzer, directly coupled to a Finnigan MAT 252 mass spectrometer. The $\delta^{15}N_{atm.N_2}$ isotope values were determined on 30 mg of ground bulk-sediment samples using the same instrument used for carbon isotope determination.

2.5. Hydrodynamic model

A 3D hydrodynamic model was set up for the late summer, covering an area of the southern Benguela upwelling system sufficiently large to include important circulation patterns around St. Helena Bay (Pitcher et al., in press). The hydrodynamics of this area were

Table 1
Site details and measured physico-chemical properties of surface sediments from St. Helena Bay

Sample id	WGS 84		Depth (m)	Sampler	Gravel (%)	Sand (%)	Mud (%)	AVS (μmol/g)	Total carbon (%)	Organic carbon (%)	Total nitrogen (%)	$\delta^{13}C$	$\delta^{15}N$
	Latitude (°S)	Longitude (°E)											
1	32.7093	17.9288	15	Grab	38.63	60.72	0.65	1	n.d	n.d	n.d	n.d	n.d
3	32.6950	17.9250	27	Multicorer	0.21	49.15	50.64	2576	5.43	1.62	0.23	n.d	n.d
4	32.6878	17.9255	31	Multicorer	0.14	64.25	35.61	1325	5.33	1.20	0.15	−19.7	5.37
5	32.5905	17.9245	58	Grab	46.25	51.99	1.76	1	n.d	n.d	n.d	n.d	n.d
6	32.5507	17.9243	66	Multicorer	0.00	96.84	3.16	358	0.84	0.50	0.11	−20.9	6.74
8	32.4258	18.0245	93	Multicorer	0.00	48.71	51.29	1287	5.12	4.74	0.63	−19.5	5.54
10	32.6015	18.0243	51	Multicorer	0.00	30.6	69.4	14062	7.19	6.24	0.81	−18.7	5.60
11	32.6727	18.0237	28	Multicorer	0.00	46.39	53.61	433	5.48	3.39	0.37	−19.4	5.82
12	32.7078	18.0240	19	Multicorer	0.14	5.90	93.96	6713	4.64	3.58	0.47	−18.9	7.19
13	32.7252	18.0233	13	Grab	32.9	27.68	39.42	1	n.d	n.d	n.d	n.d	n.d
14	32.7498	18.0280	8	Multicorer	6.7	41.9	51.4	826	5.76	2.88	0.34	−19.5	6.64
15	32.7592	18.0403	6	Multicorer	20.19	11.49	68.32	5488	5.71	4.24	0.53	−19.5	7.05
16	32.7667	18.0021	5	Multicorer	3.38	17.22	79.4	2015	5.11	3.70	0.50	−19.7	6.92
21	32.7250	18.1238	8	Multicorer	0.00	84.81	15.19	753	0.96	0.47	0.11	−18.9	5.80
24	32.5998	18.1242	32	Multicorer	n.d	n.d	n.d	11337	6.57	6.40	0.76	−18.4	5.92
26	32.4245	18.1248	72	Multicorer	0.57	13.16	86.27	9793	7.26	7.07	0.89	−18.8	4.80
27	32.4248	18.2492	48	Multicorer	0	83.25	16.75	1726	1.77	0.76	0.18	−19.2	5.71
29	32.6007	18.2485	17	Multicorer	0.44	93.88	5.68	856	0.53	0.33	0.06	−19.3	5.56
30	32.6330	18.2480	10	Multicorer	0.00	95.6	4.4	250	0.37	0.27	0.06	−19.0	6.99
31	32.6587	18.2355	6.5	Multicorer	0.00	95.87	4.13	339	0.29	0.19	0.05	−18.7	6.05
33	32.7673	18.0583	5	Multicorer	0.19	36.43	63.38	1120	4.72	2.53	0.33	−19.2	6.29
34	32.7510	18.0582	8	Multicorer	0.24	21.73	78.03	1819	3.13	2.39	0.32	−19.3	6.74
35	32.7257	18.0590	13	Multicorer	0.33	32.61	67.06	779	3.16	2.40	0.31	−19.2	6.32
36	32.7230	17.9888	8	Multicorer	0.00	79.76	20.24	707	4.46	1.59	0.18	n.d	n.d
37	32.7150	17.8460	5	Multicorer	47.61	6.57	45.82	35390	13.99	n.d	2.38	−18.8	6.22
39	32.6597	17.9807	35	Multicorer	0.00	84.07	15.93	375	2.49	0.84	0.14	−18.9	5.58
40	32.7000	17.9500	13	Multicorer	0.63	71.9	27.47	366	6.36	1.06	0.12	−19.2	5.91
42	32.4895	18.0242	80	Multicorer	0.00	23.21	76.79	567	6.98	6.46	0.85	−19.1	4.78
43	32.4923	18.1160	61	Multicorer	1.69	82.35	79.05	24874	7.40	6.56	1.63	−19.2	5.58
45	32.7522	18.0147	n.d	DiveCore	0.00	82.22	17.78	747	0.468	0.274	0.045	n.d	n.d
46	32.7766	18.1363	n.d	DiveCore	1.58	60.48	37.94	13549	2.809	2.226	0.321	n.d	n.d
47	32.7808	18.1462	n.d	DiveCore	0.00	46.8	53.2	58918	2.878	2.799	0.378	n.d	n.d
48	32.7907	18.1465	n.d	DiveCore	0.44	44.58	54.98	9526	1.373	0.833	0.198	n.d	n.d
49	32.7881	18.1687	n.d	DiveCore	0.00	75.65	24.35	1953	0.897	0.645	0.115	n.d	n.d
50	32.6968	18.1960	n.d	DiveCore	0.07	96.88	3.05	1999	0.431	0.342	0.055	n.d	n.d
51	32.7180	17.9437	n.d	DiveCore	0.00	84.08	15.92	808	8.228	0.517	0.056	n.d	n.d
52	32.7169	17.9342	n.d	DiveCore	4.24	88.96	6.8	1261	6.885	0.413	0.041	n.d	n.d

n.d., not determined.

modeled using the DELFT3D-FLOW model designed to simulate tide and wind-driven flows in shallow seas and coastal areas. A 10-layer sigma coordinate grid was used and layers were concentrated around the thermocline in order to resolve this area accurately. A curvilinear grid was designed to follow the shoreline, thus promoting a smooth flow pattern along-shore. The grid contained 130×61 lines with a variable grid cell size. At the offshore boundary, cells were as large as $8\,km \times 11\,km$, but the size was refined to approximately $60\,m \times 100\,m$ in the vicinity of St. Helena Bay and the Great Berg Estuary mouth. Overall the grid had 3202 active cells and covered a distance of approximately 240 km along-shore and 120 km cross-shore. The open boundaries were located along the three offshore edges of the model that made the southern, western and northern boundaries. At these open boundaries, a water level time-series was specified based on the predicted tide. The 8 largest amplitude tidal constituents along the west coast were applied to predict the tide (Rosenthal and Grant, 1989), which was specified at 10-min intervals. The wind data applied in the simulations were measured hourly at a St. Helena Bay weather station. The atmospheric forcing applied in the simulations included air temperature, relative humidity and cloud cover data as measured at Cape Columbine. Temperature was modeled by applying static boundary conditions at the three open boundaries. A time step of 2 min was applied. All model runs used a "cold start" with the velocity being zero everywhere. The initial sea level was set to a constant according to the initial tidal sea level specified at the open boundaries.

3. Results and discussion

3.1. Sediment biogeochemical characteristics

The measured sediment properties are given in Table 1. A majority of the sediment samples lie between the end members sand and mud, with the sand and mud content varying between 5%–96% and 1%–94%, respectively. A few samples contained gravel, where the sampling point was close or on the calcareous reefs scattered within the bay. Sediments in St. Helena Bay show a distinct distribution pattern. A tongue-shaped strip of terrigenous mud that form the southern tip of the mud belt extends from the northern to the southern edge of the bay surrounded by sand (Fig. 2a). It has been suggested that the terrigenous muds are preferentially transported south from the Orange River mouth by the subsurface poleward current (Bremner et al., 1990; Rogers and Bremner, 1991). The sandy sediments along the eastern and southern margin of the bay are thought to be contributed by the Berg River. Atmospheric dust input is far more common in the greater St. Helena Bay area and along the Namibian coast (Shannon, 1985) compared to the study area. At a number of sampled sites, the sediment–water interface was not very distinct and 1–2 cm of fluff layer, composed mostly of biogenic and fine grain coagulated sediments was observed.

The particulate organics (POC and PON) were mostly concentrated in the central region of the bay (Fig. 2b) and practically overlie on the mud belt. The organic carbon content of the sediments varied approximately between 1% and 7%, except for one sample, where 13% organic carbon was measured (Table 1). The molar C to N ratio of sediment samples was within a range of 5–9 (Fig. 2c) suggesting that most of the organic matter is of marine planktonic origin rather than from river-borne terrestrial sources (C:N > 30). Some samples showed minor carbon enrichment though, resulting in a C to N ratio as high as 11. Carbon enrichment can be associated with high productivity and high sedimentation rate regions that result in preferential carbon preservation relative to nitrogen especially in systems characterized by anoxically driven sulfidization (Brüchert et al., 2000; Twichell et al., 2002). Carbon isotope values were scattered within a narrow range of $-20.9‰$ to $-18.4‰$ (Table 1). The measured range of nitrogen isotope values was between $5.37‰$ and $7.19‰$ with lowest values occurring in the north central portion of the bay (Fig. 2d). The measured carbon and nitrogen isotope values are typical of planktonic origin.

3.2. Bulk heavy metal characteristics

In the marine environment, a number of processes have been shown to control the concentration and distribution of trace metals in sediments on a regional scale. Physical processes such as hydrodynamic flows, shelf gradient and slumping have been proposed to explain the distribution of trace metals off the coast of Ireland (Le Gall et al., 1999) and wave driven resuspension in the North Sea (Millward et al., 1998). In a comparative study of the Atlantic Ocean and the Arabian Sea, Morford and Emerson (1999) explain the variation of trace metal distribution by the change in redox state of the sediments. The role of the biological silica pump has also been highlighted in the transport and distribution of trace metals in sediments in the Southern Ocean (Löscher, 1999). In St. Helena Bay, the latter is largely discounted because of the nitrogen limitation character of the system. Similarly, redox characteristics are not the primary forcing factor but a response to the integrated hydrodynamic and biological pump scales. In retention zones associated with upwelling systems, we envision that the complex interplay of biological, chemical and physical processes that characterize their ecological importance also controls the trace metal variability and their fate.

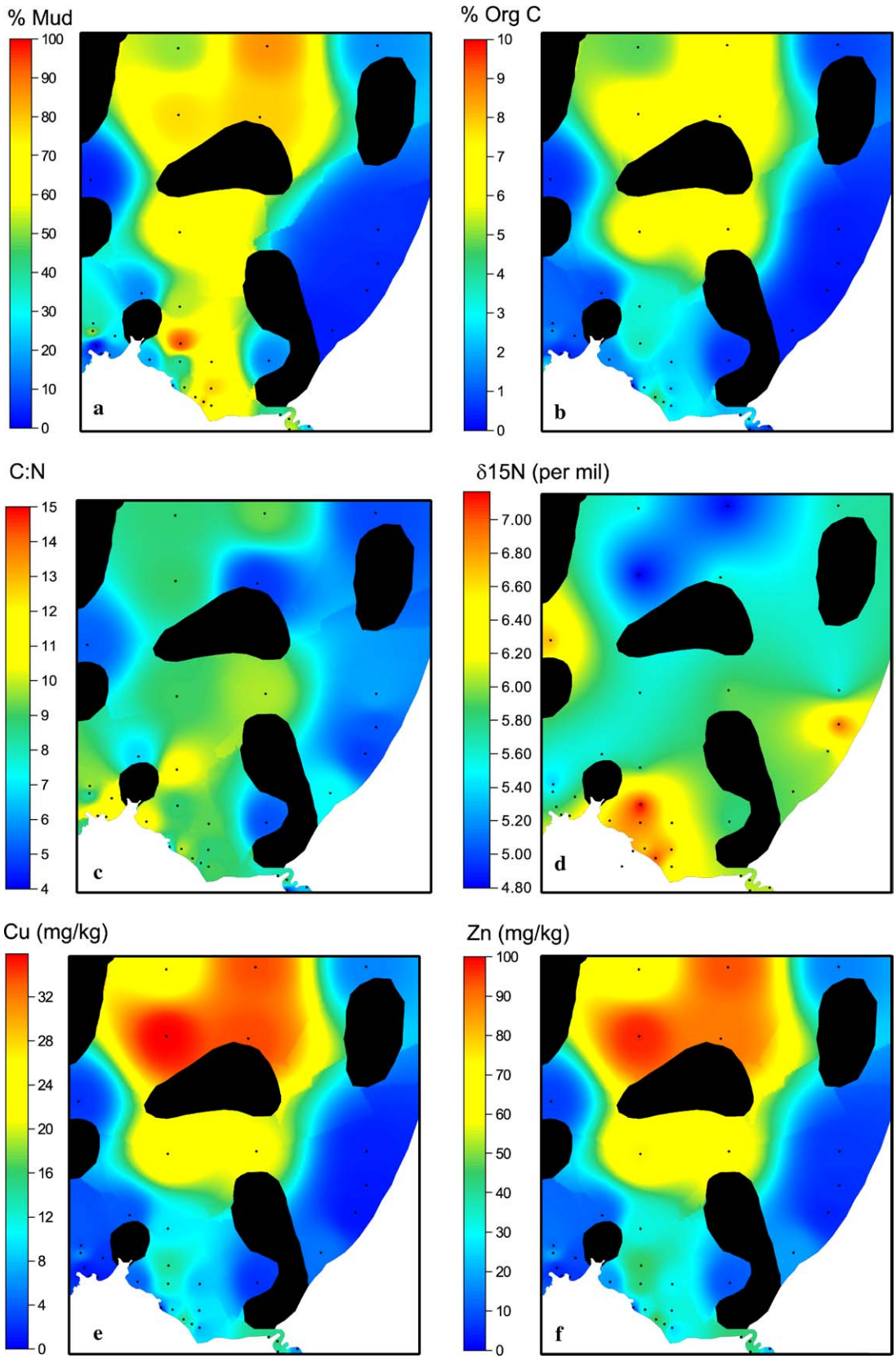

Fig. 2. Spatial distribution of selected measured properties of St. Helena Bay sediments (a) <63 μm sediment fraction (b) organic carbon content (c) carbon to nitrogen ratio (d) nitrogen isotope (e) copper and (f) zinc. Given the strong interspecies correlation, other trace metals follow the distribution pattern of copper and zinc. The contour maps were plotted based on the interpolation of spot measurements at each sampled point using Point Kriging with a linear drift.

Table 2
Trace metal concentration in bulk surface sediments collected from St. Helena Bay

Sample id	Al	Fe	Mn	Cr	Co	Ni	Cu	Zn	As	Cd	Pb
	mg/kg	mg/kg	mg/kg	mg/kg	mg/kg	mg/kg	mg/kg	mg/kg	mg/kg	mg/kg	mg/kg
1	771	1796	10.39	1.00	0.27	0.50	0.97	5.21	1.99	0.12	2.44
3	10422	7935	33.20	21.68	1.43	7.68	5.39	18.78	11.11	2.01	3.60
4	5645	5227	23.10	14.11	0.87	4.75	3.12	12.14	7.99	1.44	2.74
5	1932	3340	12.37	5.13	0.71	2.34	1.47	6.23	2.22	0.13	2.86
6	2694	28147	10.00	8.87	0.68	3.98	2.11	7.06	2.87	0.74	2.58
8	25349	19945	84.80	56.14	4.92	32.71	23.74	62.94	12.09	4.49	6.18
10	36168	24974	105.10	83.43	5.84	36.69	26.04	73.86	28.11	6.61	9.39
11	17639	11596	45.90	37.49	2.61	14.39	9.89	32.40	16.34	3.90	5.76
12	33073	21440	67.00	51.44	4.41	20.29	13.94	45.02	12.46	2.29	9.11
13	28025	17690	64.53	47.41	4.49	18.69	12.44	42.69	8.05	1.74	9.23
14	21272	14886	44.40	31.81	3.01	13.10	9.56	32.31	9.81	1.16	7.84
15	32900	21874	67.30	47.46	4.52	18.83	14.00	45.59	9.60	1.69	9.83
16	27173	19004	60.10	40.02	4.03	16.18	11.82	39.96	10.85	1.63	9.58
21	5110	3334	25.00	14.93	0.88	3.48	2.02	9.61	5.38	0.88	2.89
24	36589	23570	121.30	80.87	5.85	31.01	21.31	61.40	21.47	4.09	10.16
26	41906	31262	142.90	86.97	7.51	45.18	33.73	93.61	21.33	3.98	10.66
27	8289	4672	26.90	17.33	1.42	6.95	5.49	15.39	5.79	2.18	3.70
29	2729	1976	35.40	10.62	0.48	2.04	1.22	6.09	6.36	1.38	2.09
30	2794	1766	26.90	12.58	0.45	1.87	0.93	5.38	4.70	0.65	1.85
31	2487	1622	10.70	11.55	0.40	1.64	0.78	4.08	2.35	0.66	1.43
33	18449	11955	39.50	27.51	2.66	11.50	7.75	25.73	6.78	1.46	6.65
34	23946	15882	52.90	35.87	3.35	14.16	9.34	31.92	11.72	1.75	7.73
35	17617	11811	44.80	29.97	2.58	11.83	8.19	30.21	10.89	2.71	6.01
36	9302	7492	23.10	18.83	1.25	6.08	4.13	17.76	5.34	1.84	4.39
37	17733	11121	35.00	25.79	2.53	11.37	9.68	68.07	9.61	3.62	5.87
39	5338	3913	18.30	13.29	0.89	5.00	3.51	11.13	4.75	1.21	2.79
40	3255	4183	13.40	11.48	0.55	3.06	2.14	8.41	4.64	0.88	1.74
42	41052	30417	136.60	96.66	7.36	49.41	35.94	97.06	23.36	5.31	9.00
43	44012	31301	146.95	89.97	7.56	44.88	33.88	89.83	21.51	4.88	12.27
45	4479	3209	44.07	14.08	0.94	2.48	1.67	7.35	2.88	0.41	5.87
46	34678	21499	71.12	38.55	5.67	20.06	14.85	43.77	5.66	1.55	13.12
47	27820	20729	73.71	34.92	5.47	18.12	15.24	44.36	6.88	1.73	13.01
48	33797	20990	85.61	37.49	6.45	18.99	13.78	41.52	7.98	1.09	12.78
49	14809	9376	66.62	24.65	3.43	10.38	6.05	22.06	3.88	1.17	7.66
50	12694	8238	156.20	18.59	3.12	6.73	4.75	18.17	3.95	0.26	8.98
51	1209	1140	9.27	8.87	0.22	0.82	1.06	6.42	1.96	0.36	4.37
52	1972	1824	28.55	9.65	0.31	1.14	0.96	3.95	2.33	0.58	3.03

The bulk metal concentrations in St. Helena Bay sediments are shown in Table 2. Albeit increased pollution from urbanization, except for Cd, all trace metals (Co, Cr, Cu, Ni, Pb and Zn) have concentrations below the world average (Callender, 2003) for the near-shore sediments. In general, low trace metal concentrations are observed in the southern part of the bay and very close to the shores (Fig. 2e and f). A tongue-shaped wedge with progressively higher trace metal concentrations northward is observed between the shore and the middle of the bay, with some variations caused by the presence of the reefs. West of the central bay region, again depleted trace metal concentrations are observed (Fig. 2e and f). That is, trace metal distribution pattern, like that of organic carbon, closely follows the mud belt configuration.

Statistical analysis of trace metal data (see Table 3) suggests a strong interspecies correlation ($R > 0.70$, except for Cd and Pb) resulting in a concurrent spatial distribution of individual trace metals in St. Helena Bay. We propose that the observed relationships of trace metals are the result of their input from a common source. Furthermore, a strong linear relationship is observed between the individual trace metals and the distribution of organic carbon ($R > 0.8$, except for Mn and Pb). A somewhat weaker correlation ($R = 0.6–0.8$) is also observed between the trace metals and the mud fraction. These quantitative relationships among terrigenous fine-grained sediments, organic carbon and trace metals are clearly visible in Fig. 2a,b,e and f. However, multiple linear-regression analysis suggests that the contribution of terrigenous inorganic material towards trace metal concentrations is very small. For example, at 0% organic carbon, only 0.007 ppm copper is contributed by the terrigenous mineral fraction (see Fig. 3). Although it is possible that some trace metals are advected polewards with the terrigenous suspended mud from Orange River, based on the correlation and

Table 3
Pearson's correlation matrix for trace metals and associated physico-chemical properties of sediment from St. Helena Bay

		Gravel %	Sand %	Mud %	AVS µmol/g	Total carbon %	Organic carbon %	Total nitrogen %	Al mg/kg	Cr mg/kg	Mn mg/kg	Fe mg/kg	Co mg/kg	Ni mg/kg	Cu mg/kg	Zn mg/kg	As mg/kg	Cd mg/kg	Pb mg/kg
Gravel	**%**																		
Sand	**%**	−0.32																	
Mud	**%**	−0.16	−0.82																
AVS	**mmol/g**	0.13	−0.24	0.29															
TOC	**%**	0.61	−0.55	0.47	0.31														
OC	**%**	0.20	−0.70	0.83	0.32	0.67													
TN	**%**	0.71	−0.53	0.52	0.55	0.75	0.92												
Al	**mg/kg**	−0.09	−0.68	0.86	0.41	0.36	0.87	0.57											
Cr	**mg/kg**	−0.15	−0.57	0.80	0.29	0.43	0.96	0.59	0.92										
Mn	**mg/kg**	−0.20	−0.32	0.56	0.30	0.17	0.72	0.43	0.81	0.83									
Fe	**mg/kg**	−0.12	−0.55	0.74	0.37	0.29	0.81	0.52	0.89	0.85	0.72								
Co	**mg/kg**	−0.11	−0.58	0.77	0.44	0.29	0.83	0.53	0.98	0.91	0.87	0.89							
Ni	**mg/kg**	−0.13	−0.54	0.76	0.32	0.41	0.94	0.60	0.92	0.98	0.84	0.87	0.93						
Cu	**mg/kg**	−0.12	−0.54	0.76	0.36	0.43	0.93	0.62	0.91	0.97	0.83	0.87	0.93	1.00					
Zn	**mg/kg**	0.02	−0.64	0.78	0.45	0.56	0.94	0.78	0.91	0.94	0.80	0.85	0.91	0.96	0.97				
As	**mg/kg**	−0.17	−0.57	0.78	0.23	0.49	0.92	0.59	0.79	0.92	0.70	0.73	0.75	0.88	0.87	0.86			
Cd	**mg/kg**	−0.12	−0.48	0.67	0.30	0.55	0.88	0.69	0.71	0.86	0.61	0.66	0.69	0.85	0.84	0.86	0.93		
Pb	**mg/kg**	−0.09	−0.53	0.69	0.53	0.19	0.62	0.40	0.90	0.72	0.78	0.78	0.91	0.72	0.73	0.73	0.53	0.44	

regression, combined with sediment biogeochemical characteristics (low C:N ratios, δ^{15}N (5–7‰) and δ^{13}C (−20 to −18.4‰)) that indicate pelagic origin of POM, we suggest that phytoplankton act as the predominant common source of trace metals to the sediments in St. Helena Bay. The observed correlation between trace metals and mud fraction along with aluminum (proxy for terrigenous clays) (Table 3), is ascribed to a post depositional effect whereby the oxidation of the POC flux partitions the trace metals to adsorption sites in the clay fraction. In the long term the fate of trace metals is its partitioning between the residual organic matter, terrigenous clays and sulfide complexes.

Newly upwelled South Atlantic Central Water is thought to be the main trace metal reservoir for phytoplankton, because the river-borne flux is insignificant ($<1\ m^3\ s^{-1}$) during the upwelling season. Trace metals are scavenged by phytoplankton in the euphotic zone during growth; and deposited during the phytoplankton senescence phase. Given the shallow nature of the bay and the high senescent phase sedimentation rates ($>10\ m\ d^{-1}$) (Pitcher et al., 1989, 1991), the extent of degradation of phytoplankton during their transport through the water column is small. Therefore, trace metals are transported with the organic fraction to the surface sediments before undergoing further diagenesis.

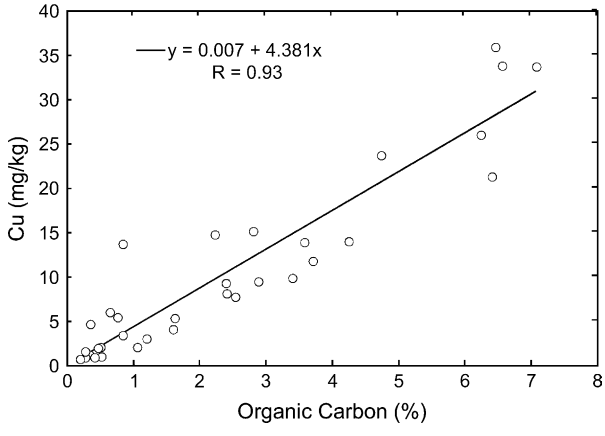

Fig. 3. The figure shows the correlation of copper, a proxy for all the measured trace metals, with organic carbon content of the sediments. The regression analysis shows that contribution of terrigenous sediments to trace metal concentration in sediments is negligible. Note that the regression analysis was carried out omitting one anomalous value of 13% for organic carbon.

A long-term Sea WiFs image (Fig. 4a) shows that the chlorophyll-*a* concentrations or surface productivity is high throughout the bay. Although this is consistent with the extent of stratified area, it also suggests that final depositional area of phytoplanktons in the bottom sediments, hence spatial distribution of trace metals, is not the same as the phytoplankton production area in the water column. Therefore, combined with the biological pump hypothesis, a central role of hydrodynamics in advection and concentration of phytoplankton within the bay waters as well as current and wave driven bed-shear stresses in the accumulation of trace metal rich organic particulates along the terrigenous mud belt is envisaged.

3.3. Hydrodynamics and productivity linkages

Upwelling, local topography and wind-driven mixing and wave refraction control the hydrodynamics within St. Helena Bay. A numerical simulation, performed for late summer shows the northward spreading of the cold ($t < 12$ °C) nutrient rich ($NO_3^- > 25\ \mu M$) waters upwelled at Cape Columbine (Fig. 4b). This cold upwelled water separates the warm offshore waters (14–15 °C)

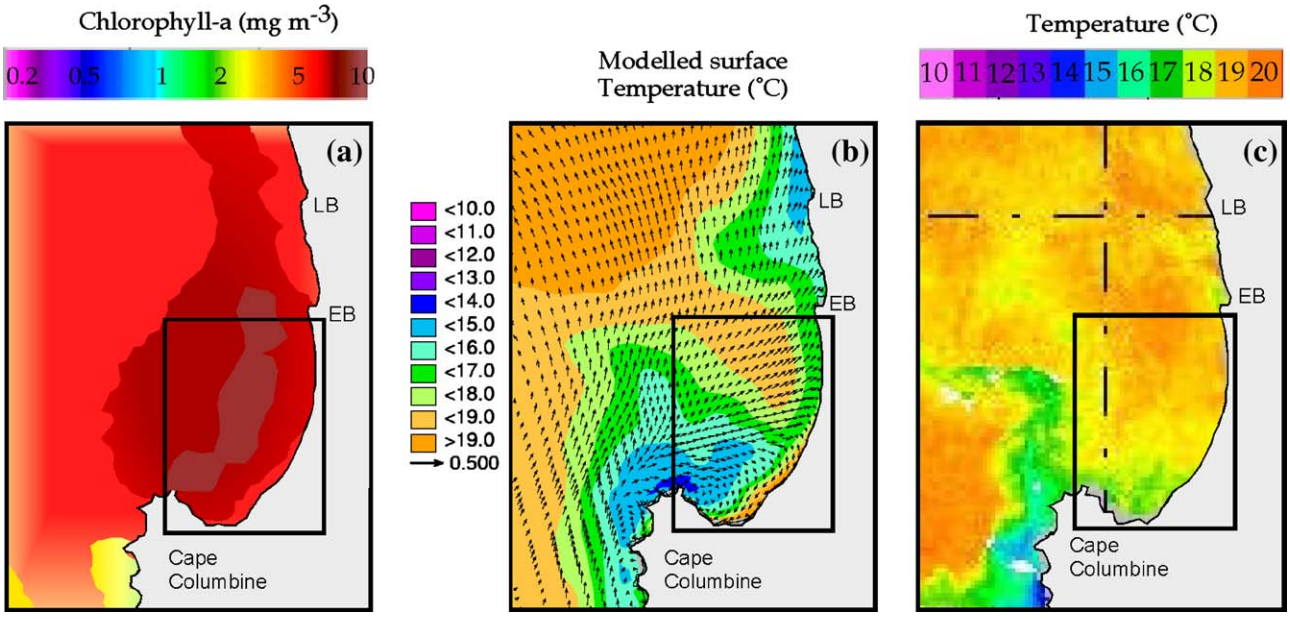

Fig. 4. (a) Mean chlorophyll-*a* concentration in St. Helena Bay redrawn from a high-resolution long-term (July 1998–June 2003) composite SeaWiFs image taken from Weeks (2005). (b) Output from a numerical simulation illustrating the temperature distribution pattern and current vectors in St. Helena Bay and surrounding regions on 26 January (c) A NOAA-AVHRR image depicting sea surface temperature for the same region and time is included for comparison. The modeled data in panel (b) shows weak inertial gyral flows and associated aged surface water in the retention zone between the offshore cold nutrient rich plume from the Cape Columbine upwelling center and the lesser near-shore upwelling. The strong vector flows of the equatorward frontal jet are clearly visible on the seaward side of the upwelled water. The inset rectangle in the three panels depicts the area sampled during this study.

from the warmer inshore surface waters (16–19 °C) in the St. Helena Bay retention zone (Fig. 4b and c). The current vector output from the numerical simulation further indicates that the circulation is dominated by inertial scales; however, there is a net residual cyclonic circulation that establishes the retention characteristics resulting in concentration inside the bay (Fig. 4b). The magnitude of retention is controlled by the wind characteristics, though (Penven et al., 2000). The modeled and observed surface temperature distribution (Fig. 4b and c) indicates a strong stratification within St. Helena Bay with warm surface waters underlain by cold upwelled water. The strength of the stratification governs the rate of local surface phytoplankton new production supported by turbulent diffusion of nutrients across the thermocline (Monteiro et al., 1998; Monteiro and Largier, 1999). However, summer stratification is also strongly modulated by wind-driven entrainment periods, when both cooling and nutrient enrichment of the surface layer dominates. Such an entrainment event occurred on 4–6 February 2002 when the temperature difference between the surface layer and the cold upwelled water decreased by 5 °C (Fig. 5). The subsequent gradual stratification resulted in the growth and subsequent senescence of a dense algal bloom that led to a mass mortality event of rock lobster in the first few days of March 2002 (unpublished data). Blooms resulting from these entrainment events are gradually starved of nutrient supply as stratification intensifies and are concentrated within the retention zone via the cyclonic gyre where they rain out rapidly (Pitcher et al., 1991).

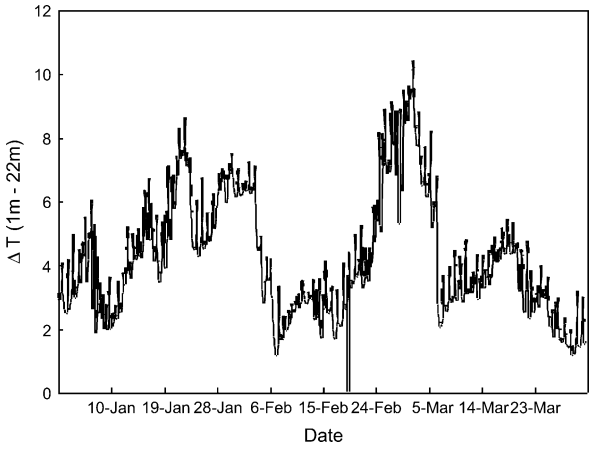

Fig. 5. The variability of a stratification proxy (surface layer – bottom layer temperature, ΔT) over the late summer period in 25 m deep water on the western side of St. Helena Bay retention zone. Temperature data was measured using an Anderaa thermistor chain with a 2 m resolution and logging at a 30 min interval. Variability on a time scale of hours–days shows how temperature is modulated by the dynamics of sun warming and wind-driven entrainment cooling. The illustrated episodic mixing and stratification highlights the importance of the event scale with respect to new production and its sedimentation flux.

The observed (1–5 g $C\,m^{-2}\,d^{-1}$) (Bailey, 1987) and modeled (1–7 g $C\,m^{-2}\,d^{-1}$) (Touratier et al., 2003) organic carbon flux in St. Helena Bay is higher than what could be accounted for by new production alone (0.4–0.6 g $C\,m^{-2}\,d^{-1}$) (Waldron and Probyn, 1991; Probyn, 1992; Monteiro et al., 1998). That is, there is a net positive flux of organic carbon into the bay to supplement local production, highlighting the role of hydrodynamics in transporting particulate material from outside the boundaries of the bay. Alternating upwelling and relaxation conditions force and enhance retention by strengthening the cross shelf flow as well as the near-shore poleward flow that transports external blooms into the retention zone where they are concentrated (Probyn et al., 2000; Pitcher et al., in press). The integrated biomass distribution predicted by such an import – retention conceptual model in the system is reflected by a long-term composite SeaWiFs image (Fig. 4a). The image shows that the distribution of new production derived biomass is in close agreement with the spatial scale of the stratified area of the system but larger than the spatial scale of the terrigenous mud belt (Fig. 4a). This suggests that the spatial scale of the mud belt, where particulate organic matter and associated trace metals accumulate is determined by both the area of sedimentation, as well as by seabed turbulence dynamics. Bed-shear stresses, which govern the re-suspension and deposition dynamics of fine sediments and biogenic particles, are driven by bottom friction effects from both the summer barotropic jet ($>0.5\,m\,s^{-1}$) on the western boundary (Fig. 4b) and by the winter storm wave bed stresses that reflect on the shallow eastern boundary (Monteiro et al., 1999). The re-suspension fluxes resulting from these temporally mismatched forcing processes add to the depositional load of organic material on the terrigenous mud belt.

The integrated characteristics of the coupled hydrodynamic–biological pump hypothesis that is proposed to govern sediment elemental biogeochemistry in St. Helena Bay are synthesized in Fig. 6. A barotropic jet, associated with the Benguela upwelling current, vertically transports cold nutrient rich water and trace metals on the western margin of the St. Helena Bay. Part of the upwelled water is advected laterally into the bay below the thermocline. The primary productivity in the photic zone, hence uptake of trace metals, depends on the exchange of nutrients and trace metals between the cold nutrient rich bottom waters and warm surface layer through eddy diffusion and mixing across the thermocline. The mixing, and thereby the exchange process, is enhanced during wind entrainment events associated with the strong South-Eastern winds during the summer months. Newly formed organic matter is retained within the bay because of the creation of a retention area by the presence of the barotropic jet on the western margin and associated residual cyclonic currents that concentrate new production at the northern margin and transport it southwards. Dead organic matter along with suspended particulate matter transported poleward is deposited at the bottom across the bay. Once deposited, sediments

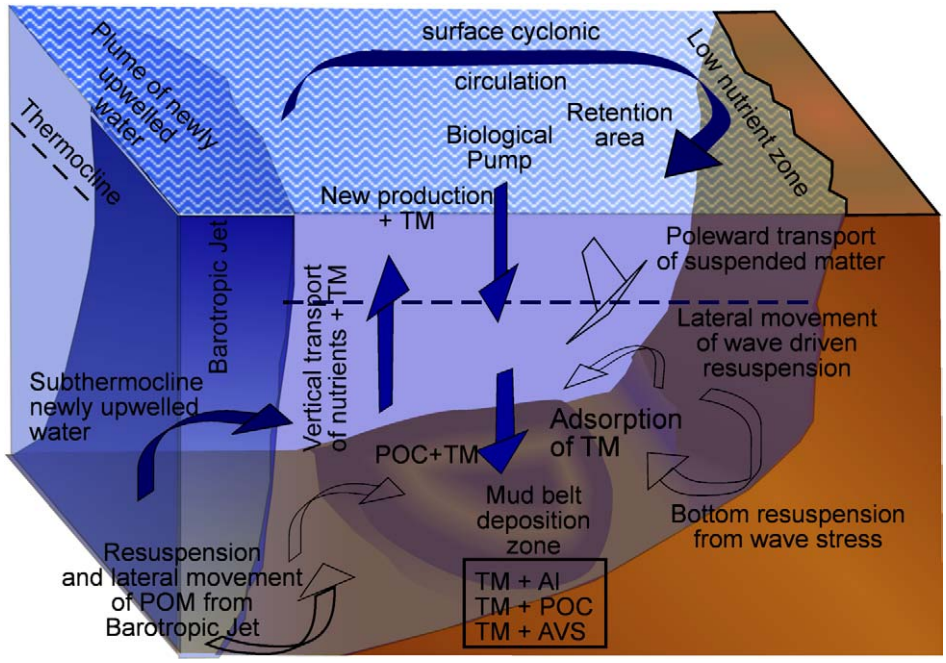

Fig. 6. A schematic diagram outlining the major biogeochemical and hydrodynamic processes that control the production, retention and depositional characteristics within the St. Helena Bay.

are further subjected to re-suspension and are laterally transported in almost opposite directions by the barotropic jet at the western margin, and wave reflection from the land margins during the winter storms. This results in the deposition of the sedimentary load along a narrow belt, thereby imparting the unique spatial characteristics observed in the sediment biogeochemistry of St. Helena Bay.

4. Summary

Wind-driven upwelling plays a significant role in controlling the biogeochemical processes occurring along the west coast of Southern Africa. In retention zones, the cold, nutrient rich water drives the biological pump and hydrodynamics play a major role in the transport and fate of organic matter and trace elements. In order to understand trace metal dynamics in St. Helena Bay, the following characteristics, linking the water column processes with the sediment, must be emphasized:

- trace metals brought into the coastal waters of St. Helena Bay through upwelling are primarily assimilated by new production;
- a flux of upwelled nutrients drives the productivity that links the particulate flux of organic matter and associated trace metals to the sediment reservoir;
- the particulate flux is enhanced by concentration of surface layer productivity within the retention zone by a weak cyclonic gyre driven by alternating upwelling and relaxation periods;
- the spatial scale of phytoplankton sedimentation does not match the depositional area of the mud belt where organics and trace metals ultimately are accumulated;
- the near bottom turbulence regimes brought about by winter wave driven shear stresses along the eastern margin and the barotropic jet on the western boundary defines the near-shore and offshore boundaries of the trace metal accumulation areas.

Acknowledgement

This project was supported by research funds from NRF-SIDA, NRF (Grant # 2054021) and URC, University of Cape Town. The authors are grateful to Mr Andrew Pascal for his help with field logistics and sampling and to Ms Anel Kemp for creating the model output figure. The authors wish to thank two anonymous journal reviewers who provided constructive criticisms and comments on the manuscript, and to Dr Eric Wolanski for handling the manuscript.

References

Bailey, G.W., 1987. The role of regeneration from the sediments in the supply of nutrients to the euphotic zone in the southern Benguela system. South African Journal of Marine Science 5, 273–286.

Bailey, G.W., 1991. Organic carbon flux and development of oxygen deficiency on the modern Benguela continential shelf south of 22°S spatial and temporal variability. In: Tyson, R.V., Pearson, T.H. (Eds.), Modern and Ancient Continental Shelf Anoxia, pp. 171–183.

Bakun, A., 1998. Ocean triads and radical interdecadal stock variability: bane and boon for fisheries management. In: Pitcher, T., Hart, P.J.B., Pauly, D. (Eds.), Reinventing Fisheries Management. Chapman and Hall, pp. 331–358.

Bremner, J.M., Rogers, J., Willis, J.P., 1990. Sedimentological aspects of the 1988 Orange River floods. Transactions of the Royal Society of South Africa 47, 247–294.

Brüchert, V., Pérez, M.E., Lange, C.B., 2000. Coupled primary production, benthic foraminiferal assemblage, and sulfur diagenesis in organic-rich sediments of the Benguela upwelling system. Marine Geology 163, 27–40.

Callender, E., 2003. Heavy metals in the environment – historical trends. In: Lollar, B.S. (Ed.), Treaties on Geochemistry: Environmental Geochemistry, vol. 9. Elsevier Ltd., pp. 67–105.

Chapman, P., Bailey, G.W., 1991. Short-term variability during an anchor station study in the southern Benguela upwelling system. Progress in Oceanography 28, 1–7.

Chapman, P., Shannon, L.V., 1985. The Benguela ecosystem. Part II. Chemistry and related processes. Oceanography and Marine Biology: An Annual Review 23, 183–251.

Cockroft, A., Schoeman, D.S., Pitcher, G.C., Bailey, G.W., van Zyl, D.C., 2000. A mass stranding of west coast rock lobster Jasus lalandii in Elands Bay, South Africa; causes, results and applications. In: Von Kaupel Klein, J.C., Schram, F.R. (Eds.), The Biodiversity Crises and Crustaceans, vol. 11, pp. 362–368 (Crustacean Issues).

Fisher, N.S., Wente, M., 1993. The release of trace elements by dying marine phytoplankton. Deep-Sea Research I 40 (4), 671–694.

Fourie, J.M., Steer, A.G., 1971. Water quality survey of the Berg River for the period 1963 to 1970. National Institute for Water Research, South Africa.

González-Dávila, M., 1995. The role of phytoplankton cells on the control of heavy metal concentration in seawater. Marine Chemistry 48, 215–236.

Graham, W.M., Largier, J.L., 1997. Upwelling shadows as nearshore retention sites: the example of northern Monterey Bay. Continental Shelf Research 17, 509–532.

Hudson, R.J.M., Morel, F.M.M., 1993. Trace metal transport by marine microorganisms: implications of metal coordination kinetics. Deep-Sea Research I 40 (1), 129–150.

Hutchings, L., 1992. Fish harvesting in a variable, productive environment. South African Journal of Marine Science 12, 297–318.

Jones, S.E., Jago, C.F., Bale, A.J., Chapman, D., Howland, R.J.M., Jakson, J., 1998. Aggregation and resuspension of suspended particulate matter at a seasonally stratified site in the southern North Sea: physical and biological controls. Continental Shelf Research 18 (11), 1283–1310.

Le Gall, A.C., Statham, P.J., Morley, N.H., Hydes, D.J., Hunt, C.H., 1999. Processes influencing distribution and concentration of Cd, Cu, Mn and Ni at the North West European shelf break. Marine Chemistry 68, 97–115.

Löscher, B.M., 1999. Relationship among Ni, Cu, Zn, and major nutrients in the Southern Ocean. Marine Chemistry 67, 67–102.

Millward, G.E., Morris, A.W., Tappin, A.D., 1998. Trace metals at two sites in the southern North Sea: results from a sediment resuspension study. Continental Shelf Research 18 (11), 1381–1400.

Monteiro, P.M.S., Largier, J.L., 1999. Thermal stratification in Saldanha Bay, South Africa, and sub-tidal, density driven exchange with coastal waters of the Benguela upwelling system. Estuarine, Coastal and Shelf Science 49 (6), 877–890.

Monteiro, P.M.S., Pascall, A., Brown, S., 1999. The Biogeochemical Status of Surface Sediments in Saldanha Bay in 1999. CSIR, Stellenbosch, South Africa.

Monteiro, P.M.S., Spolander, B., Brundrit, G.B., Nelson, G., 1998. Shellfish mariculture in the upwelling systems: estimates of nitrogen driven new production using two physical models. Journal of Shellfish Research 17 (1), 3–13.

Monteiro, P.M.S., van der Plas, A.K. Forecasting low oxygen water (LOW) variability in the Benguela System. In: Shannon, L.V., Woods, J., Moloney, C.L. (Eds.), The Benguela and Comparable Systems. Elsevier, in press.

Morel, F.M.M., Price, N.M., 2003. The biogeochemical cycles of trace metals in the oceans. Science 300, 944–947.

Morford, J.L., Emerson, S., 1999. The geochemistry of redox sensitive trace metals in sediments. Geochimica et Cosmochimica Acta 63 (11/12), 1735–1750.

Nelson, G., Hutchings, L., 1983. The Benguela upwelling area. Progress in Oceanography 12, 333–356.

Noriki, S., Ishimori, N., Harada, K., Tsunogai, S., 1985. Removal of trace metals from seawater during a phytoplankton bloom as studied with sediment traps in Funka Bay, Japan. Marine Chemistry 17, 75–89.

Penven, P., Roy, C., Colin de Verdiere, A., Largier, J.L., 2000. Simulation of a coastal jet retention process using a barotropic model. Oceanologica Acta 23 (5), 616–634.

Pitcher, G.C., Brown, P.C., Mitchell-Innes, B.A., 1992. Spatio-temporal variability of phytoplankton in the southern Benguela upwelling system. South African Journal of Marine Science 12, 439–456.

Pitcher, G.C., Monteiro, P.M.S., Kemp, A.J. The potential use of a hydrodynamic model in the prediction of harmful algal blooms in the southern Benguela. In: Steidinger, K. (Ed.), Harmful and Toxic Algal Blooms. Intergovernmental Oceanographic Commission of UNESCO, in press.

Pitcher, G.C., Walker, D.R., Mitchell-Innes, B.A., 1989. Phytoplankton sinking rate dynamics in the southern Benguela upwelling system. Marine Ecology-Progress Series 55, 261–269.

Pitcher, G.C., Walker, D.R., Mitchell-Innes, B.A., Moloney, C.L., 1991. Short-term variability during an anchor station study in the southern Benguela upwelling system: Phytoplankton dynamics. Progress in Oceanography 28, 39–64.

Probyn, T.A., 1992. The inorganic nitrogen nutrition of phytoplankton in the southern Benguela: new production, phytoplankton size and implications for pelagic foodwebs. In: Payne, A.I.L., Brink, K.H., Mann, K.H., Hilborn, R. (Eds.), Benguela Trophic Functioning. South African Journal of Marine Science 12, 411–420.

Probyn, T.A., Pitcher, G.C., Monteiro, P.M.S., Boyd, A.J., Nelson, G., 2000. Physical processes contributing to harmful algal blooms in Saldanha Bay, South Africa. South African Journal of Marine Science 22, 285–298.

Rogers, J., Bremner, J.M., 1991. The Benguela ecosystem. Part VII. Marine-geological aspects. Oceanography and Marine Biology Annual Review 29, 1–85.

Rosenthal, G., Grant, S., 1989. Simplified tidal prediction for the South African coastline. South African Journal of Science 85, 104–107.

Roy, C., 1998. Upwelling-induced retention area: a mechanism to link upwelling and retention processes. South African Journal of Marine Science 19, 89–98.

Shannon, L.V., 1985. The Benguela ecosystem, Part I. Evolution of the Benguela, physical features and processes. Annual Reviews in Oceanography and Marine Biology 23, 105–182.

Shannon, L.V., Nelson, G., 1996. The Benguela: large scale features and processes and system variability. In: Wefer, G., Berger, W.H., Siedler, G., Webb, D. (Eds.), The South Atlantic: Present and Past Circulation. Springer-Verlag.

Touratier, F., Field, J.G., Moloney, C.L., 2003. Simulated carbon and nitrogen flow of the planktonic food web during an upwelling relaxation period in St Helena Bay (southern Benguela ecosystem). Progress in Oceanography 58, 1–41.

Twichell, S.C., Meyers, P.A., Diester-Haass, L., 2002. Significance of high C/N ratios in organic-carbon-rich Neogene sediments under the Benguela Current upwelling system. Organic Geochemistry 33, 715–722.

Vasconcelos, M.T.S.D., Leal, M.F.C., van den Berg, C.M.G., 2002. Influence of the nature of the exudates released by different marine algae on the growth, trace metal uptake and exudation of *Emiliania huxleyi* in natural seawater. Marine Chemistry 77, 187–210.

Waldron, H.N., Probyn, T.A., 1991. Short term variability during an anchor station study in the southern Benguela upwelling system: nitrogen supply to the euphotic zone during a quiescent phase of the upwelling cycle. Progress in Oceanography 28, 153–166.

Wangersky, P.J., 1986. Biological control of trace metal residence time and speciation: a review and synthesis. Marine Chemistry 18, 269–297.

Weeks, S.J., 2005. Specific applications of satellite remote sensing to the Benguela Ecosystem. PhD thesis, University of Cape Town, South Africa.

Whitfield, M., 2001. Interaction between phytoplankton and trace metals in the ocean. Advances in Marine Biology 41, 1–128.